A gold-bearing volcanogenic-exhalative horizon in the Archaean(?) Saqqaq supracrustal rocks, Nuussuaq, West Greenland

Adam A. Garde, Bjørn Thomassen, Tapani Tukiainen and Agnete Steenfelt

The Saqqaq supracrustal rocks in southern Nuussuaq, West Greenland, host stratiform gold mineralisation in a 3–4 m thick impure chert horizon of volcanogenic-exhalative origin; chip samples average *c.* 0.8 ppm Au (thickness 3.3 m) over a strike length of 8 km, including 1.1 ppm Au (thickness 3.7 m) over a strike length of 1.6 km. Silicate minerals in and adjacent to the mineralised horizon include chrome-bearing tourmaline, staurolite, fuchsite, and manganiferous garnet. The Saqqaq supracrustal rocks form an almost 30 km long, NW-striking and SW-dipping sequence, which is presumed to be of Archaean age and consists of amphibolite facies mafic and ultramafic metavolcanic rocks, associated minor volcanogenic-exhalative horizons, and quartzo-feldspathic metasediments. The sequence is surrounded by Archaean(?) orthogneisses and intruded by an up to *c.* 100 m thick trondhjemitic sill, and appears to outline a large asymmetric, isoclinal fold (possibly of Archaean age) which was refolded in the lower Proterozoic.

Geological Survey of Denmark and Greenland, Thoravej 8, DK-2400, Copenhagen NV, Denmark.
E-mail: *aag@geus.dk.*

Keywords: Archaean, gold, Nuussuaq, supracrustal rocks, West Greenland

In 1986 a large unit of previously unknown supracrustal rocks was discovered in the Precambrian basement of southern Nuussuaq near the settlement of Saqqaq (Fig. 1) during helicopter reconnaissance of Tertiary basalt outliers (A.K. Pedersen, personal communication 1988). The unit was subsequently investigated during the Disko Bugt Project 1988–92 carried out by the Geological Survey of Greenland (GGU; see Kalsbeek & Christiansen 1992). Initial analyses of stream sediment and sulphide mineralised samples from the supracrustal unit showed enrichment in arsenic and traces of gold, and subsequent chip sampling revealed the existence of a several kilometres long gold-bearing horizon. In 1992 Platinova A/S investigated the supracrustal belt during two weeks of field work, which mainly comprised chip sampling of rusty horizons.

This paper presents the currently available, although somewhat sketchy knowledge of the mineralisation and its host rocks. It is based on reconnaissance geological and geochemical mapping in 1988, 1989 and 1991 (Steenfelt 1992; Garde & Steenfelt 1999, this volume) and chip sampling in 1991 (Thomassen & Tukiainen 1992), geological photogrammetry, microscope studies and whole-rock and mineral geochemistry by the authors, as well as mineralisation data obtained by Platinova A/S (Atkinson & Rutherford 1992). As will be seen below, the gold mineralisation at Saqqaq differs in many respects from the one at Eqi south-east of Nuussuaq (likewise studied during the Disko Bugt Project) which is related to carbonate alteration in Archaean acid metavolcanic rocks (Stendal *et al.* 1999, this volume).

Geology

The Saqqaq supracrustal rocks (Garde 1994) form a NW–SE-striking, *c.* 29 km long and up to *c.* 5 km wide belt (Fig. 1) which is enclosed in the Precambrian orthogneiss complex of southern Nuussuaq and locally capped by basaltic flows of Tertiary age. The supracrustal belt, which generally dips 25–40° SW, is more than 500 m thick, but its original base and top have not been recognised. The entire belt may form a recumbent isoclinal fold as suggested by large-scale, flat-lying isoclinal folds with north-west-trending axes

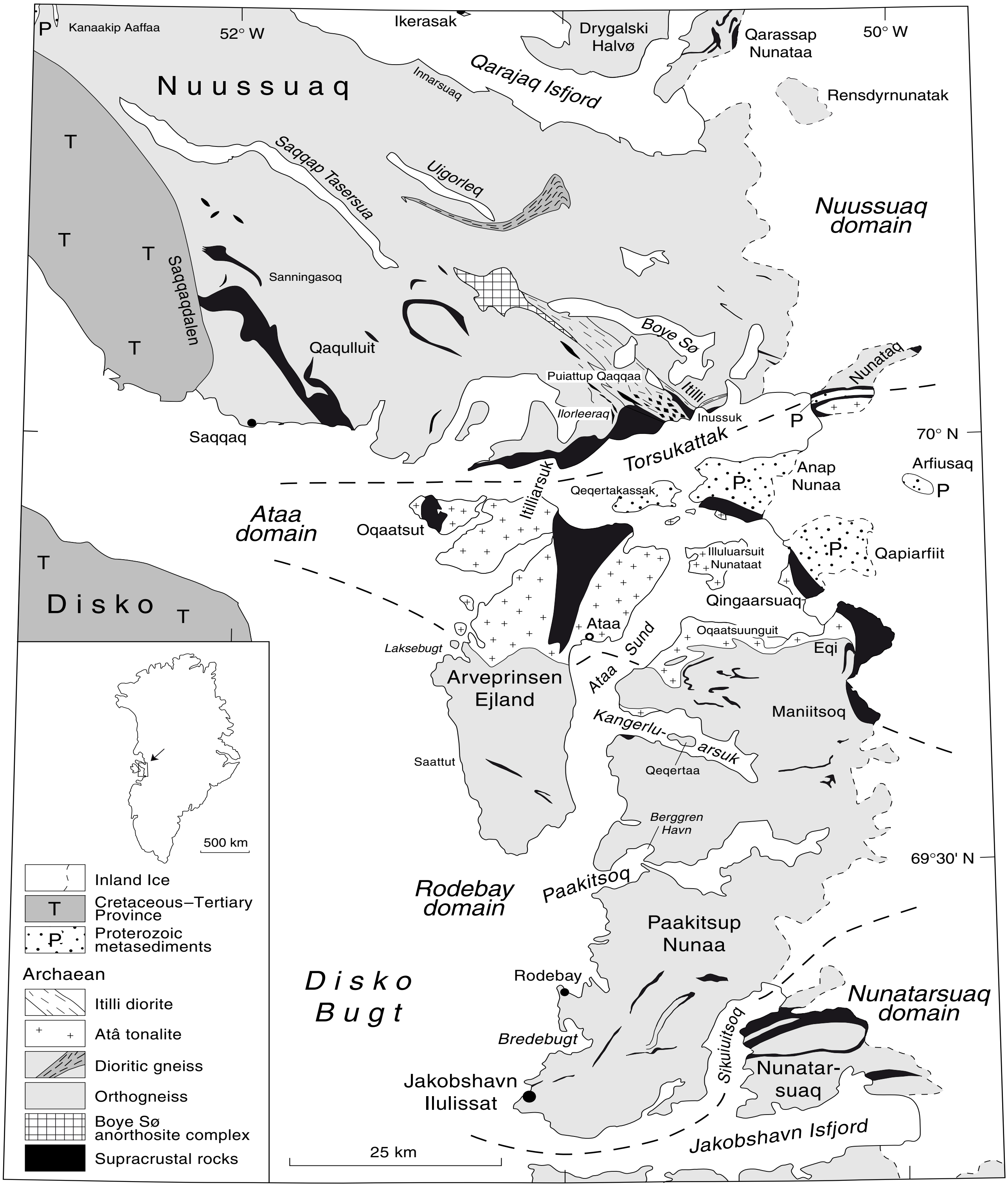

Fig. 1. Simplified geological map showing the Saqqaq supracrustal rocks, the auriferous metachert horizon with chip sample analyses (ppb Au and width in metres), locations of other rust zones, and the position of Fig. 3. The supracrustal sequence continues to the coast south-east of the map area.

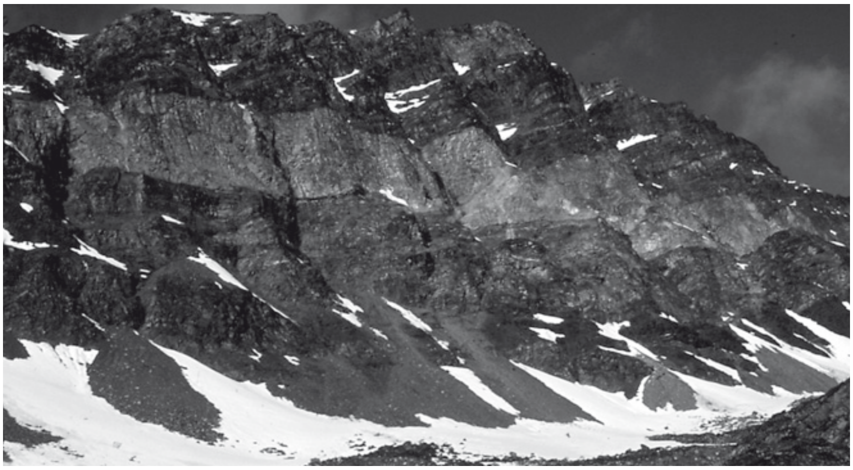

Fig. 2. Photograph of the central part of a NE-facing cliff face opposite the mountain Qaqulluit (Figs 1, 3), displaying a section through part of the Saqqaq supracrustal rocks with the rusty metachert (*c.* 30 m thick) horizon above the scree. The light grey layer in the upper part of the picture is a trondhjemitic sill; the uppermost part of the succession is not visible due to the short distance between the observer and the cliff face (compare the section made by geological photogrammetry, Fig. 3).

visible, e.g. on the cliffs north and south of the lake Iluliallip Tasia. The south-eastern end of the supracrustal belt has been folded into an upright antiform with a subhorizontal north-west-trending axis during a later phase of deformation, presumably in the Proterozoic (Garde & Steenfelt 1999, this volume). Medium- and small-scale fold structures are common in the supracrustal rocks, but their relationship with the large-scale structures is uncertain. Smaller enclaves of supracrustal rocks are common in the gneisses in the vicinity of the supracrustal belt to the north and west.

Exposures of relatively undisturbed supracrustal rocks occur in a NE-facing, up to *c.* 500 m high, steep mountain wall opposite the mountain Qaqulluit (Figs 2, 3). This slope was mapped and interpreted using multi-model geological photogrammetry (Dueholm 1992) based on photography from a helicopter (Fig. 3). The lowermost parts accessible by foot have been traversed and sampled (Fig. 4). The supracrustal sequence in the slope generally dips 30° SW. Exposures of the basement-cover contact between the supracrustal sequence and the regional orthogneiss have not

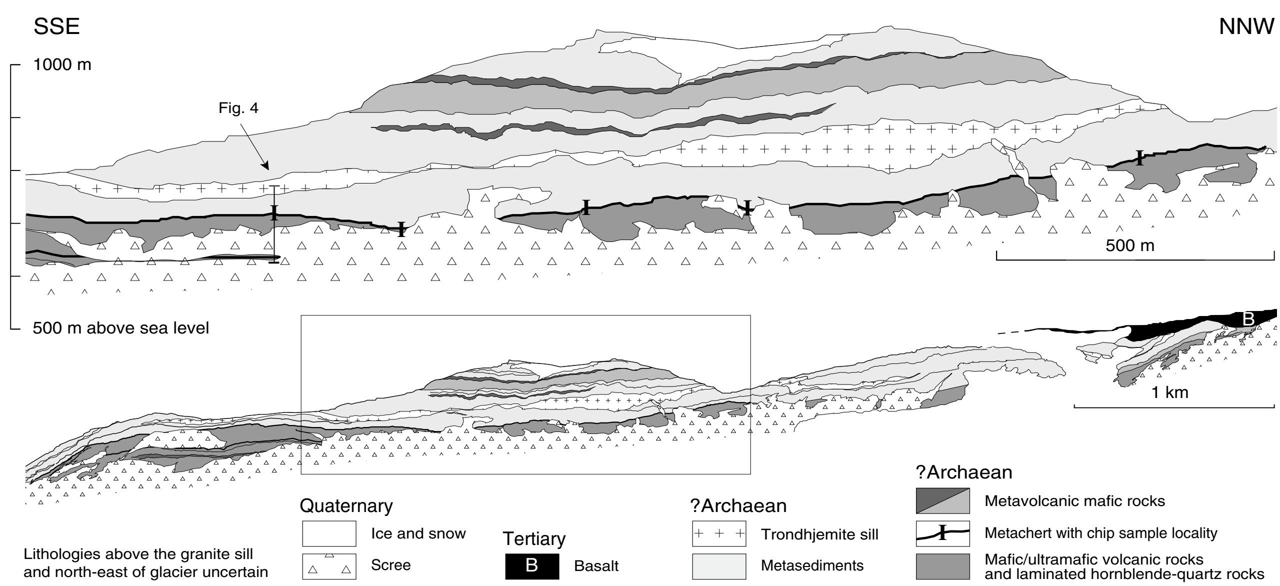

Fig. 3. Saqqaq supracrustal rocks exposed along a 6 km long NE-facing cliff face opposite the mountain Qaqulluit. Direction of view WSW (240°). See Fig. 1 for location and compare with the photograph Fig. 2. Geological interpretation and topography based on geological photogrammetry, supplemented with observations by foot from short traverses at the chip sampled localities. The lithologies indicated above the trondhjemitic sill and north-east of the glacier are uncertain.

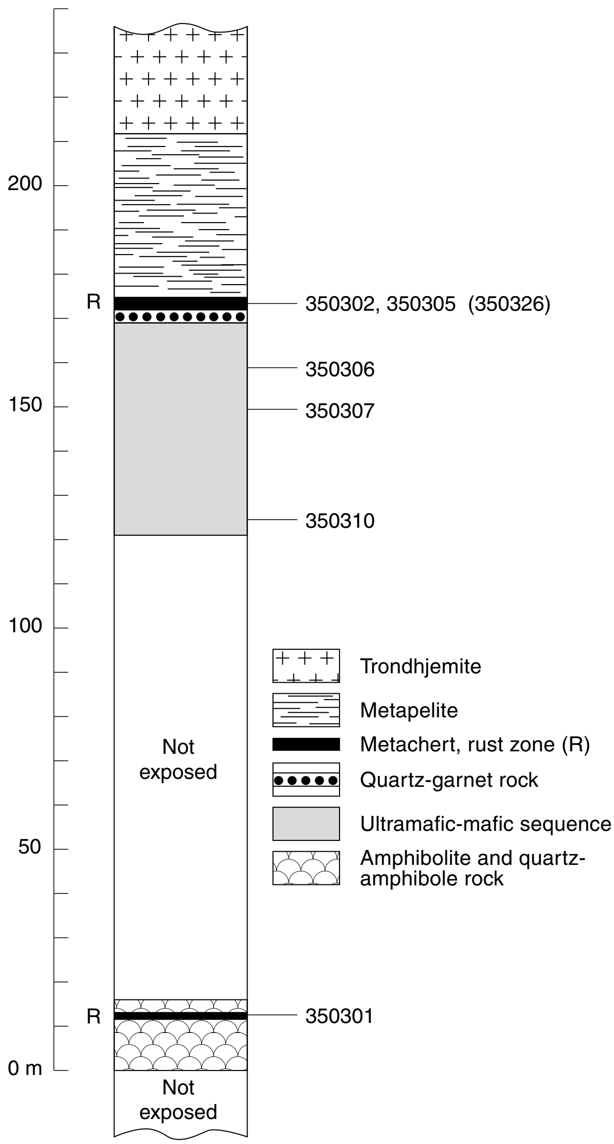

Fig. 4. Stratigraphic section of the lower part of the Saqqaq supracrustal rocks opposite the mountain Qaqulluit (Fig. 3 for location), and stratigraphic positions of samples referred to in the text and Table 1. 350301: Amphibole-quartz-garnet-tourmaline-pyrrhotite rock. 350302, 350305: Impure metachert. 350306–350307: Laminated hornblende-quartz rock. 350310: Ultrabasic metavolcanic rock. 350326: Amphibole-quartz-pyrrhotite rock (local block collected from scree immediately below the auriferous impure metachert and rusty garnet-rich horizon).

been observed by the present authors but were reported by Platinova A/S as strongly sheared and commonly mineralised with iron sulphides (see p. 125).

The lowermost outcrops, protruding between the scree fans that generally cover the lower parts of the slopes (Figs 3, 4), consist of a dark green to black, fine-grained amphibolite and very finely laminated quartz-amphibole rock. The latter rock type consists of monomineralic bands of quartz and amphibole which alternate at a scale of 0.1–0.5 mm, besides thin scattered stringers of pyrite and pyrrhotite. Within these rocks an up to 1.5 m thick, fine-grained, rusty horizon contains a number of several millimetres thick layers consisting of hornblende, plagioclase, biotite, quartz, garnet, tourmaline, pyrrhotite and ilmenite in varying proportions.

The next exposed unit consists of an ultramafic-mafic sequence with a true thickness of more than 60 m. It is composed of ultrabasic metavolcanics, which are intercalated with dark olive-green hornblendite and laminated quartz-hornblende rocks. The lowermost exposed part of this unit consists of a massive, brown-weathering, strongly carbonated ultrabasic rock. In places it displays a decimetre-sized meshwork texture that may be interpreted as partially recrystallised coarse spinifex structure; alternatively it was formed during metamorphic recrystallisation. The ultrabasic rock mostly consists of fine-grained intergrowths of chlorite, tremolite and serpentine, often with substantial amounts of dolomite and magnetite, besides sporadic pyrrhotite and pyrite. There are also local 2–4 cm thick monomineralic lenses of *c.* 0.5 cm large, equidimensional olivine grains, cut by thin serpentine veins. The olivine grains are magnesian and very homogeneous (Fo_{86}, Table 1), and the lenses are interpreted as inherited from the pre-metamorphic protolith. Upwards in the outcrop the dark green laminated hornblende-rich horizons increase in frequency and thickness (millimetres to decimetres) so that eventually they become the predominant rock type. They consist mainly of fine-grained quartz and actinolitic to ferro-tschermakitic hornblende with low but variable sodium and potassium contents (Fig. 5; Table 1).

The ultramafic-mafic sequence is overlain by two thin but conspicuous horizons of supposed volcanic-exhalative origin (see below). The lower one, a rusty weathering garnet-rich horizon with variable thickness up to 1.5 m, is greyish and conspicuously banded at a scale of millimetres to centimetres. The mineralogical composition of this rock is quartz, garnet, fuchsite, biotite, chlorite, colourless amphibole, titanite and tourmaline, along with minor ilmenite, pyrrhotite, niccolite, wolframite and scheelite. It is rich in aggregates and 1–5 cm thick monomineralic layers of up to 2 cm large euhedral garnet porphyroblasts with colours varying from dark red to almost black. The garnets contain many small pyrrhotite inclusions and are almandine-rich. The garnets also contain up to *c.* 10 wt per cent

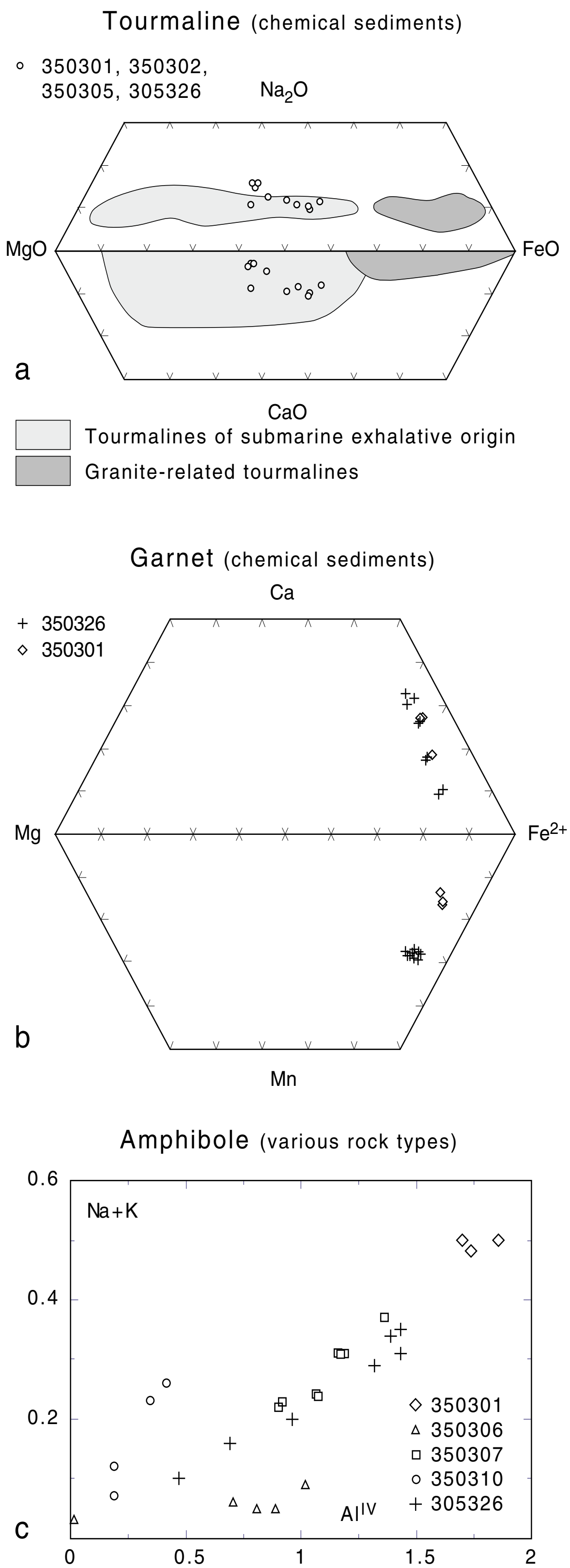

MnO (Fig. 5; Table 1); manganese-rich garnet is a characteristic component of coticule (quartz-spessartine rock) which is commonly interpreted as a volcanogenic-exhalative sea floor precipitate (Gardiner & Venugopal 1992 and references therein).

The second conspicuous horizon has a distinct lower contact to the garnet-rich horizon, is 3–4 m thick, rusty weathering, and consists of finely laminated, impure metachert with occasional small-scale folds with near-horizontal, NW-striking axes. Quartz is the predominant mineral, followed by pyrrhotite and fuchsite, and smaller amounts of one or more of the following minerals: biotite, chlorite, garnet, actinolitic hornblende, titanite, tourmaline, staurolite, tremolite, pyrite, arsenopyrite; native gold (electrum, see p. 126) has also been identified. Several of the silicate minerals (chlorite, fuchsite, staurolite, tourmaline) contain Cr_2O_3 in the range 0.5–2.0 wt per cent (Table 1), whereas chromite has not been identified. The tourmaline is intermediate in composition between dravite and schorl (Fig. 5). Like the quartz-amphibole rocks lower in the section, the metachert is mostly very fine grained and finely laminated, with widely separated trains of single grains of one or several of the above mentioned minerals. Some samples contain microfolds at a scale of centimetres, within which the fine lamination is preserved, but where pyrrhotite has been partially remobilised into thin stringers along axial surfaces. A few metachert samples have been recrystallised and appear coarser and much less distinctly banded.

The metachert horizon is succeeded upwards by *c.* 40 m of slightly migmatised, grey, fine-grained rocks consisting of quartz, plagioclase, biotite, muscovite, garnet and chlorite, and traces of pyrite. This sequence is

Fig. 5. Compositions of tourmaline, garnet and amphibole in chemical sediments, and amphibole in an ultrabasic metavolcanic rock. See Fig. 4 for sample locations and lithologies.
a: Na_2O–MgO–FeO and CaO–MgO–FeO triangular diagrams of tourmaline in chemical sediments. Comparison with compositional fields of tourmalines with known origins (from Henry & Guidotti 1985) support our interpretation that the sediments are of submarine-exhalative origin. **b**: Ca–Mg–Fe^{2+} and Mn–Mg–Fe^{2+} triangular diagrams of garnet in chemical sediments; their large iron and particularly manganese contents are reminiscent of coticule garnet. **c**: Variation diagram of amphiboles, Na + K plotted against Al in IV-coordination per unit cell. The diagram illustrates the large variation of amphibole compositions found in chemical sediments (samples 350301, 350306–07, 350326) and the low coupled substitution of Al^{IV} and Na, K for Si^{4+} in tremolite from the ultrabasic metavolcanic rock (sample 350310).

Table 1. Compositions of silicate minerals from chemical sediments and metavolcanic rocks, Saqqaq supracrustal rocks

	Garnet				Tourmaline				Amphibole								
GGU	350301	350326	350326	350326	350301	350302	350305	350326	350301	350306	350307	350307	350307	350310	350310	350326	350326
No	average	55	average	s.d.	average	average	average	average	average	e3	f59	av. (g)	s.d.	average	s.d.	b30	c34
Spot	n = 3		n = 8		n = 2	n = 2	n = 3	n = 3	n = 2			n = 4		n = 3			
SiO_2	37.55	37.43	37.15	0.15	34.96	35.24	35.11	34.68	41.84	51.22	46.14	48.87	1.40	56.02	0.97	52.57	44.47
TiO_2	0.05	0.01	0.02	0.03	1.13	0.49	0.42	1.37	0.48	0.24	0.32	0.29	0.02	0.01	0.00	0.18	0.57
Al_2O_3	21.47	20.92	21.22	0.30	31.94	32.00	31.62	31.28	15.56	6.21	10.61	8.25	1.22	1.65	0.80	3.67	12.66
Cr_2O_3	0.08	0.09	0.04	0.03	0.07	1.72	2.16	0.03	0.02	0.49	0.73	0.58	0.41	0.04	0.05	0.02	0.05
FeO*	27.91	26.02	24.21	1.86	7.97	5.46	5.70	8.02	18.61	11.69	12.35	11.84	0.47	2.77	0.10	12.45	15.45
MgO	1.62	1.90	1.70	0.35	6.65	7.46	7.49	6.62	6.91	14.87	13.56	14.42	0.93	23.02	0.15	15.36	10.03
MnO	5.23	10.70	10.07	0.79	0.14	0.01	0.10	0.19	0.20	0.27	0.26	0.20	0.13	0.17	0.03	0.45	0.34
NiO	0.01	0.05	0.03	0.03	0.03	0.09	0.04	0.02	0.03	0.05	0.19	0.22	0.04	0.08	0.01	0.02	0.01
CaO	7.37	2.69	5.89	2.62	1.38	0.81	0.51	1.53	11.74	11.90	11.51	12.12	0.16	12.47	0.16	12.60	11.89
Na_2O	0.03	0.04	0.04	0.05	1.92	2.00	2.22	1.69	1.26	0.14	1.16	0.87	0.13	0.75	0.26	0.31	0.85
K_2O	0.04	0.01	0.02	0.02	0.01	0.07	0.03	0.08	0.67	0.11	0.28	0.07	0.04	0.03	0.03	0.07	0.58
Sum	101.37	99.87	100.39	0.58	86.18	85.34	85.41	85.49	97.30	97.18	97.12	97.72	0.79	97.01	0.39	97.69	96.90
Fe_2O_3	0.96	0.00	0.99	0.72					2.72	5.42	7.89	5.21	0.29	3.08	0.12	2.90	3.73
FeO	27.05	26.02	23.32	2.08					16.17	6.81	5.25	7.15	0.70	0.00	0.00	9.84	12.09
New sum	101.47	99.87	100.49	0.64					97.60	97.73	97.90	98.25	0.03	97.32	0.01	97.99	97.27
Cations per formula unit																	
Si	5.94	6.06	5.95	0.05	5.79	5.82	5.81	5.79	6.28	7.29	6.64	6.98	0.12	7.68	0.12	7.53	6.57
Al	4.00	3.99	4.00	0.05	6.23	6.23	6.17	6.16	2.75	1.04	1.80	1.39	0.19	0.27	0.13	0.62	2.20
Ti	0.01	0.00	0.00	0.00	0.14	0.06	0.05	0.17	0.05	0.03	0.03	0.03	0.00	0.00	0.00	0.02	0.06
Cr	0.01	0.01	0.01	0.01	0.01	0.22	0.29	0.00	0.00	0.06	0.08	0.07	0.04	0.00	0.01	0.00	0.01
Fe^{2+}	3.58	3.52	3.12	0.29	1.10	0.75	0.79	1.12	2.03	0.81	0.63	0.85	0.10	0.00	0.00	1.18	1.49
Fe^{3+}	0.11	0.00	0.12	0.08	0.00	0.00	0.00	0.00	0.31	0.58	0.85	0.56	0.03	0.32	0.01	0.31	0.41
Mn	0.70	1.47	1.37	0.11	0.00	0.00	0.00	0.00	0.03	0.03	0.03	0.02	0.02	0.02	0.00	0.05	0.04
Ni	0.00	0.01	0.00	0.01	0.00	0.00	0.00	0.00	0.00	0.01	0.02	0.03	0.01	0.01	0.00	0.00	0.00
Mg	0.38	0.46	0.41	0.09	1.64	1.84	1.85	1.65	1.55	3.16	2.91	3.07	0.16	4.70	0.02	3.28	2.21
Ca	1.25	0.47	1.01	0.45	0.25	0.14	0.09	0.28	1.89	1.81	1.77	1.85	0.01	1.83	0.02	1.93	1.88
Na	0.01	0.01	0.01	0.02	0.62	0.64	0.71	0.55	0.37	0.04	0.32	0.24	0.04	0.20	0.07	0.09	0.24
K	0.01	0.00	0.00	0.00	0.00	0.01	0.01	0.02	0.13	0.02	0.05	0.01	0.01	0.01	0.01	0.01	0.11
Total	6.00	16.00	16.00	0.00	15.77	15.72	15.77	15.73	15.38	14.87	15.15	15.11	0.04	15.04	0.07	15.03	15.23
Oxygens	24.00	24.05	24.00						23.00	23.00	23.00	23.00		22.91	0.02	23.00	23.00

Note the high chromium content in chlorite, tourmaline, staurolite and fuchsitic muscovite in several samples. The samples were collected along the profile shown in Fig. 4.

The analyses were made with the Jeol 733 Superprobe at the Geological Institute, University of Copenhagen. The electron microprobe was operated at 15 kV, 15 nA with energy dispersive data collection (major elements except Na) and crystal spectrometers (Na, Cr, Ni), and a beam diameter of 2 mm. Natural silicates and oxides of end-member compositions were used as standards.

Iron distribution of Fe_2O_3 and FeO according to isometric requirements.

interpreted as sedimentary or volcano-sedimentary in origin.

The uppermost accessible unit in the section is a prominent, *c.* 50 m thick sheet of whitish, slightly foliated trondhjemite. The rock is homogeneous and medium grained, and appears to be more leucocratic than the country rock tonalitic gneisses. Hand samples show that it has been strained during regional deformation. However, the photogrammetric interpretation (Fig. 3) clearly suggests that it is transgressive, which is supported by occasional observations of aplitic veins in the supracrustal sequence that emerge from the trondhjemite sheet. The upper, steep part of the mountain wall has not been traversed, but the supracrustal rocks appear to continue for another *c.* 200 m above the trondhjemite sill to the top of the mountain (Fig. 3).

In the north-facing cliffs south of the lake Iluliallip Tasia (Fig. 1), rock types similar to the ones at Qaqulluit were observed, and also here a gold-bearing, rusty-weathering horizon of metachert was identified and sampled in the lower part of the section. This metachert is considered to be continuous with the one at Qaqulluit, although there are structural complexities in the upper part of the section; the east–west section through the supracrustal belt suggests the presence of a large recumbent, NE-facing fold with a horizontal axis directed SE. North of the lake, the supracrustal rocks are strongly deformed by disharmonic folding, so that a clear stratigraphic section through the unit is not apparent. Ultramafic and mafic rocks predominate

Table 1 (*continued*)

	Biotite				Muscovite			Chlorite		Serpentine		Staurolite	Olivine	
GGU No	350301	350301	350307	350307	350302	350305	350305	350305	350310	350310	350310	350302	350310	350310
Spot	average	s.d.	average	s.d.	average	37	42	43	b	13	14		average	s.d.
	n = 4		n = 3		n = 2				n = 2			n = 2	n = 3	
SiO_2	34.70	0.70	34.97	0.48	45.23	46.74	48.02	24.41	32.29	42.01	39.95	26.94	39.93	0.08
TiO_2	1.86	0.18	2.64	0.14	0.62	0.42	0.51	0.01	0.14	0.01	0.01	0.62	0.01	0.00
Al_2O_3	17.26	0.11	15.95	0.34	33.36	35.28	30.68	22.08	14.96	0.01	0.01	52.73	0.01	0.00
Cr_2O_3	0.08	0.06	0.61	0.05	0.79	0.80	0.57	0.23	0.56	0.01	0.02	1.06	0.01	0.00
FeO^*	21.82	0.48	14.87	0.38	1.99	2.36	2.93	20.88	4.10	2.44	4.67	11.73	13.37	0.17
MgO	9.68	0.24	15.65	0.33	0.58	0.45	0.75	17.26	33.43	42.64	40.84	1.22	45.73	0.06
MnO	0.20	0.14	0.18	0.15	0.14	0.13	0.01	0.30	0.01	0.01	0.01	0.35	0.25	0.08
NiO	0.01	0.00	0.35	0.05	0.02	0.01	0.01	0.16	0.18	0.25	0.26	0.06	0.29	0.03
CaO	0.05	0.07	0.06	0.09	0.01	0.01	0.16	0.01	0.19	0.01	0.01	0.07	0.01	0.00
Na_2O	0.07	0.03	0.35	0.05	1.14	0.93	1.11	0.01	0.02	0.01	0.01	0.01	0.01	0.00
K_2O	8.23	0.82	7.18	0.50	8.84	7.95	8.59	0.01	0.01	0.01	0.01	0.01	0.09	0.10
Sum	93.93	1.27	92.81	0.89	92.70	95.09	93.33	85.35	85.88	87.41	85.80	94.78	99.71	0.25
Fe_2O_3					2.21	2.62	3.26	0.52	0.67					
FeO					0.00	0.00	0.00	20.42	3.49					
New sum					92.92	95.35	93.66	85.40	85.95					
Cations per formula unit														
Si	5.55	0.04	5.47	0.02	3.08	3.08	3.24	5.18	6.20	1.95	1.90	3.94	1.00	0.00
Al	3.25	0.06	2.94	0.04	2.68	2.74	2.44	5.52	3.39	0.00	0.00	9.10	0.00	0.00
Ti	0.23	0.02	0.31	0.02	0.03	0.02	0.03	0.00	0.02	0.00	0.00	0.07	0.00	0.00
Cr	0.01	0.01	0.08	0.01	0.04	0.04	0.03	0.04	0.09	0.00	0.00	0.12	0.00	0.00
Fe^{2+}	2.92	0.11	1.94	0.06	0.00	0.00	0.00	3.62	0.56	0.09	0.19	1.44	0.28	0.00
Fe^{3+}	0.00	0.00	0.00	0.00	0.11	0.13	0.17	0.08	0.10	0.00	0.00	0.00	0.00	0.00
Mn	0.03	0.02	0.02	0.02	0.01	0.01	0.00	0.05	0.00	0.00	0.00	0.04	0.01	0.00
Ni	0.00	0.00	0.04	0.01	0.00	0.00	0.00	0.03	0.03	0.01	0.01	0.01	0.01	0.00
Mg	2.31	0.07	3.65	0.11	0.06	0.04	0.08	5.46	9.57	2.95	2.90	0.27	1.71	0.00
Ca	0.01	0.02	0.01	0.02	0.00	0.00	0.01	0.00	0.04	0.00	0.00	0.01	0.00	0.00
Na	0.02	0.01	0.11	0.02	0.15	0.12	0.15	0.00	0.01	0.00	0.00	0.00	0.00	0.00
K	1.68	0.15	1.43	0.09	0.77	0.67	0.74	0.00	0.00	0.00	0.00	0.00	0.00	0.00
Total	16.00	0.00	16.00	0.00	6.82	6.71	6.70	20.00	20.00	5.00	5.00	15.00	3.00	0.00
Oxygens	45.12	0.11	45.03	0.05	11.00	11.00	11.00	28.00	28.00	6.95	6.90			

here, and the gold-bearing metachert horizon was only recognised in one small outcrop.

The lithologies and structures in the northernmost and southernmost parts of the supracrustal belt have not been studied by the authors.

Mineralisation

In the Saqqaq supracrustal rocks sulphide mineralisation occurs in four different settings: (1) in metavolcanic rocks which are almost devoid of gold, (2) in siliceous shear zones with low gold contents at contacts between the host orthogneiss and supracrustal rocks, (3) in quartz-garnet rock with an unusual sulphide paragenesis and elevated gold contents, and (4) in metachert, the main gold-bearing association.

The metavolcanic rocks contain a number of rust zones with disseminated to semi-massive pyrrhotite and pyrite and traces of chalcopyrite. Analyses of five chip samples from such mineralised zones are summarised in Table 2. It is evident that the contents of gold (average 12 ppb) and base metals are modest. Similar results were obtained by Platinova A/S: 18.5 ppb Au on average for 20 samples (Atkinson & Rutherford 1992). Analysis of a number of mineralised boulders confirms this picture of a rather pure iron sulphide mineralisation. Only one boulder of chalcopyrite-bearing ultramafic rock from the northern shore of Iluliallip Tasia with 0.3% Cu and 235 ppb Au deviates from this pattern.

Mineralisation at gneiss–supracrustal rock contacts was described by Atkinson & Rutherford (1992), according to whom this is the most common type of mineralisation and probably the most extensive. The contact zones are highly silicified (recrystallised?) and intensely banded, presumably mylonitic. Sulphide contents vary from trace to 50 per cent over 1–2 m. Pyrrhotite is dominant, but in addition pyrite, arsenopyrite, chalcopyrite, galena and sphalerite are present in trace to minor amounts. Gold contents are low, 30 ppb in average for 36 chip samples.

Table 2. Summary of mineralisation geochemistry in the Saqqaq supracrustal rocks

	Metavolcanic rocks 5 chip samples			Quartz-garnet rock 1 grab sample	Metachert 8 chip samples		
	Min.	Max.	Mean		Min.	Max.	Mean
Width m	1.0	5.0	2.1		1.5	4.5	3.3
SiO_2	48.3	55.3	50.8	51.3	66.5	87.1	78.8
TiO_2	0.4	1.3	0.7	1.7	0.2	0.5	0.3
Al_2O_3	8.3	14.3	11.1	18.6	2.8	6.8	4.1
Fe_2O_3	15.5	21.1	18.1	20.2	3.8	15.2	10.3
MnO	0.3	0.6	0.4	0.6	0.1	0.4	0.2
MgO	3.4	6.9	4.7	3.9	0.5	3.0	2.0
CaO	2.5	9.3	7.2	0.6	0.1	3.1	1.0
Na_2O	0.4	1.9	0.9	0.2	0.1	0.4	0.2
K_2O	0.1	0.6	0.4	2.2	0.1	1.7	0.6
P_2O_5	0.1	0.1	0.1	0.1	<0.1	0.1	<0.1
Au ppb	1	38	12	116	95	1831	757
Ag ppm	<5	<5	<5	<5	<5	<5	<5
As ppm	<2	190	45	1800	9	1600	404
W ppm	<4	11	6	46	<4	15	8
Ni ppm	<50	470	109	1800	<50	1500	652
Co ppm	19	70	45	150	9	110	66
Pt ppb	<5	7	5	<5	<5	6	5
Pd ppb	<2	7	3	2	3	9	5
Cr ppm	180	1000	376	240	120	2800	1403
Cu ppm	150	498	268	21	64	406	137
Zn ppm	20	104	55	27	9	42	19
Pb ppm	16	114	43	2	12	52	20
Sb ppm	<0.2	<0.2	<0.2	93.0	<0.2	29.0	9.4
Ba ppm	79	292	133	184	35	130	61

Analysis by Activation Laboratories Ltd., Ontario.
Major elements (%): fusion-inductivity coupled plasma emission spectrometry (icp).
Au, Pt, Pd: fire assay-icp.
Cu, Zn, Pb: aqua regia extraction-icp.
Ag, As, W, Ni, Co, Cr, Sb, Ba: instrumental neutron activation.

The quartz-garnet rock contains *c.* 1 vol.% of disseminated, fine-grained sulphides: niccolite, gersdorfite, pentlandite and pyrrhotite, as well as wolframite, scheelite and ilmenite. The pentlandite occurs as isolated, monomineralic grains, i.e. it is not formed by exsolution from pyrrhotite. The mineralogy is reflected by the chemical analyses (Table 2), which shows relatively high contents of nickel, arsenic and tungsten, as well as antimony and gold (116 ppb).

The auriferous metachert horizon contains a few volume per cent disseminated, fine-grained sulphides. Loose blocks indicate that semi-massive sulphide concentrations do occur, but none have been observed in outcrop. The main sulphide minerals are pyrrhotite and pyrite, accompanied by minor arsenopyrite and chalcopyrite. A tendency to lateral pyrite-pyrrhotite zonation with an increase of pyrrhotite towards NW has been observed. Grains of native gold up to 20 µm in size occur both as inclusions in arsenopyrite and as single isolated grains (Fig. 6). Energy dispersive microprobe analysis of three gold grains in arsenopyrite indicates a uniform Au/Ag ratio of 61/37, i.e. strictly speaking the mineral is electrum.

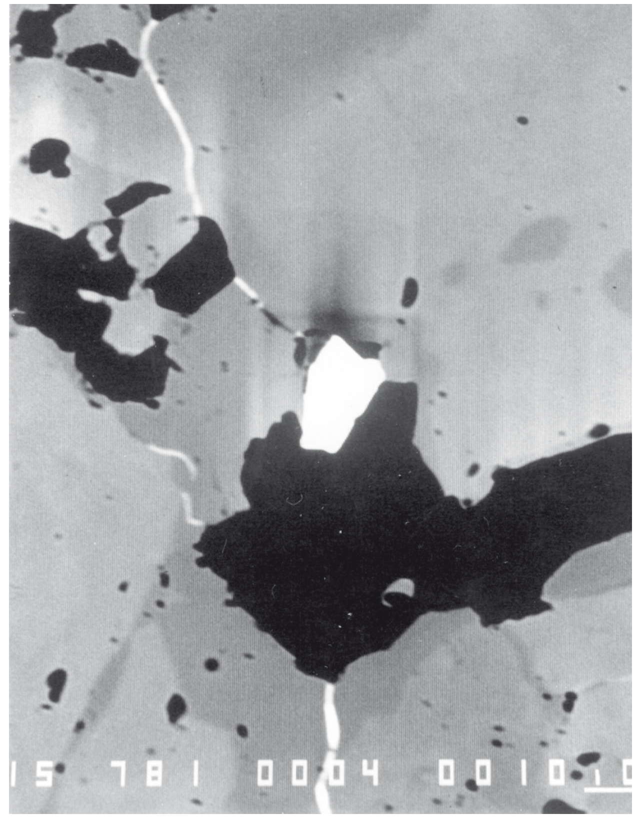

Fig. 6. Backscatter photomicrograph of gold (electrum) in the auriferous metachert, filling cracks and cavities in arsenopyrite. The gold grain in the centre (white) is *c.* 20 µm in diameter.

The metachert horizon was chip sampled (*c.* 3 kg samples) at eight localities along a lateral distance of *c.* 8.5 km (Figs 1, 3). Analyses of these samples are summarised in Table 2 (average 757 ppb Au over a width of 3.3 m) and suggest that the entire horizon is enriched in gold. The five chip samples from opposite Qaqulluit alone, collected over a strike length of 1.6 km, average 1063 ppb Au over a width of 3.7 m. Comparable values were obtained by Platinova A/S with an average of 663 ppb Au in 20 chip samples; the best result, opposite Qaqulluit, was an average of 1896 ppb Au in five samples over a lateral extent of 500 m (Atkinson & Rutherford 1992). The auriferous horizon is also enriched in arsenic (hosted in arsenopyrite), nickel (hosted in both sulphides and silicates), chromium (apparently hosted mainly in silicates) and antimony, whereas base metal contents are rather low (Table 2).

Sphalerite and galena are only known from boulders at two localities near Iluliallip Tasia where they occur in veined rocks, perhaps originally chert, and in vein quartz respectively. The boulders contain up to 1.6 wt per cent Zn, 1.2% Pb, 0.1% Cu, 62 ppm Ag and 247 ppb Au.

Discussion

Most of the rocks studied in thin section exhibit equilibrium textures, with the exception of the ultrabasic metavolcanic rock where deformed lenses of medium-grained olivine occur in a fine-grained chlorite-tremolite-carbonate-serpentine matrix. The composition of the olivine, which appears to be very homogeneous, is shown in Table 1. The composition of the olivine (Fo_{86} and 0.29 wt% NiO) is similar to what might be expected in a fresh picritic or komatiitic lava, and together with the textures suggest to the authors that the olivines are primary and have survived later events without significant recrystallisation or chemical modification. Peak metamorphic temperature and pressure conditions of low to middle amphibolite facies are estimated from the coexisting hornblende and plagioclase (An_{38}), the common presence of biotite, almandine-rich garnet, staurolite and titanite in mafic rocks, as well as from the general composition of the calcic amphiboles which show only limited Al + Na, K substitution for Si (Fig. 5) and low TiO_2 contents. Apart from sporadic growth of late chlorite the examined rocks do not contain much evidence of recrystallisation after the peak of metamorphism.

Both the amphibole-quartz(-garnet) rocks and the metachert horizons are mostly very finely laminated, at a scale down to a fraction of a millimetre. The laminations may be rhythmic with alternating microlayers of two different mineralogical compositions (e.g. quartz-fuchsite or quartz-amphibole), but in the case of the metacherts also more complex variations may occur. For instance, several narrow zones rich in tourmaline crystals, or trains of single tourmaline or staurolite crystals may occur at variable intervals within the same thin section of metachert. The metachert often contains microfolds outlined by the lamination, and sometimes the folds are associated with recrystallisation which blurs the lamination. We therefore consider that the fine laminations in these rocks were formed by primary sedimentation and precipitation processes on the sea floor, and have survived subsequent metamorphism and deformation. This interpretation is in contrast to Atkinson & Rutherford (1992) who, from field observations, argue that the horizon represents a mylonitised shear zone analogous to the ones they observed along contacts between orthogneiss and supracrustal rocks. However, given the presence of an extensive, serpentinised and hence very ductile ultrabasic horizon close by, we consider it unlikely that the metachert should represent a siliceous mylonite zone.

The incomplete knowledge of the Saqqaq supracrustal rocks does not allow for a detailed account of their formation. A predominantly volcanic subaqueous depositional setting is indicated, which comprises a sequence of subaqueous ultramafic and mafic lavas changing upwards into pyroclastic and exhalative deposits and finally into volcaniclastic or epiclastic sediments. These rocks, probably deposited in a subsiding trough, were subsequently affected by deformation, metamorphism and metasomatism, and were intruded by a granitoid sill. Garde & Steenfelt (1999, this volume) correlate the Saqqaq supracrustal rocks with a supracrustal unit comprising similar lithologies in southern Nuussuaq 30–50 km further to the east and argue that both supracrustal units are Archaean and were formed in a back-arc or active continental margin setting.

The quartz-hornblende rocks of the metavolcanic unit, the quartz-garnet rock and the auriferous metachert most likely represent exhalative deposits formed on the sea floor by chemical precipitation from discharged metalliferous hydrothermal brines. Presumably the hydrothermal activity was contemporaneous with the ultramafic-mafic submarine volcanism. Our interpretation is supported by the composition of tourmalines from the metachert, which in a MgO–FeO–CaO–Na_2O diagram (Fig. 5) plot in the field of tourmalines supposed to have formed by chemical precipitation (Henry & Guidotti 1985). Likewise, the manganese-rich composition of garnets in the quartz-garnet rock is reminiscent of coticule of supposed volcanogenic exhalative origin (Gardiner & Venugopal 1992). Upwards in the sequence the volcanic-pyroclastic component decreases, resulting in a nearly pure exhalative deposit, the auriferous metachert horizon. The relative enrichment of the minor elements arsenic, chromium, nickel, tungsten and boron in the latter horizon is typical for gold mineralisation in Archaean greenstone belts (Hutchinson & Burlington 1984) and points towards a contribution from the ultramafic-mafic lavas.

Gold deposits hosted by chemical sediments including As-bearing sulphide-silicate iron formations are important in Archaean greenstone belts on a worldwide scale, e.g. at Lupin (Canada), Homestake (USA) (Thorpe & Franklin 1984), and in the Zimbabwe Craton (Saager *et al.* 1987). In general the gold is partly uniformly disseminated in the host units and partly located in minor quartz veins, which may be irregularly distributed or structurally controlled. Various authors (e.g. Sawkins & Rye 1974; Hutchinson & Burlington 1984) have proposed that the initial gold mineralisation is syngenetic from hydrothermal exhalations in chemical sediments on the sea floor. Subsequent folding, metamorphism and intrusion of granitoids causes remobilisation of gold into the quartz lodes so characteristic for this mineralisation, but which have not yet been discovered in the Saqqaq area. Others have stressed the epigenetic nature of most Archaean gold deposits (Groves & Foster 1991); certainly ore-grade gold mineralisation is mostly associated with quartz veins, as found for example in the Lupin district where the bulk of the gold is hosted by alteration haloes related to pervasive quartz veining (Bullis *et al.* 1994).

The auriferous metachert of the Saqqaq supracrustal rocks seems to be compatible with the syngenetic model outlined above, although a more comprehensive conclusion must await further studies. At this stage it appears that the economic potential of the Saqqaq supracrustal rocks lies in primary gold concentrations in the metachert horizon rich enough to be mineable, with additional potential for the discovery of epigenetic quartz vein gold derived from the metachert. We also emphasise that large parts of the area underlain by the Saqqaq supracrustal rocks remain untested and certainly warrant investigation.

Acknowledgements

We are grateful to J. Rønsbo, Geological Institute, University of Copenhagen, for assistance with the microprobe analysis. The Danish Natural Science Research Council funded the microprobe facilities.

References

Atkinson, J.R. & Rutherford, R. 1992: Report on 1992 field program, Saqqaq concession, West Greenland, 26 pp. Unpublished report, Platinova A/S, Toronto, Canada (in archives of Geological Survey of Denmark and Greenland).

Bullis, H.R., Hureau, R.A. & Penner, B.D. 1994: Distribution of gold and sulfides at Lupin, Northwest Territories. Economic Geology **86**, 1217–1227.

Dueholm, K.S. 1992: Geological photogrammetry using standard small-frame cameras. In: Dueholm, K.S. & Pedersen, A.K. (eds): Geological analysis and mapping using multi-model photogrammetry. Rapport Grønlands Geologiske Undersøgelse **156**, 7–18.

Garde, A.A. 1994: Precambrian geology between Qarajaq Isfjord and Jakobshavn Isfjord, West Greenland, 1:250 000. Copenhagen: Geological Survey of Greenland.

Garde, A.A. & Steenfelt, A. 1999: Precambrian geology of Nuussuaq and the area north-east of Disko Bugt, West Greenland. In: Kalsbeek, F. (ed.): Precambrian geology of the Disko Bugt region, West Greenland. Geology of Greenland Survey Bulletin **181**, 6–40 (this volume).

Gardiner, W.W. & Venugopal, D.V. 1992: Spessartine-quartz rock (coticule) occurrences in New Brunswick, Canada, and their use in exploration for massive sulphide, tin-tungsten and gold deposits. Transactions of the Institution of Mining and Metallurgy, Section B: Applied Earth Science **101**, B147–B157.

Groves, D.I. & Foster, R.P. 1991: Archaean lode gold deposits. In: Foster, R.P. (ed.): Gold metallogeny and exploration, 63–103. Glasgow & London: Blackie.

Henry, D.J. & Guidotti, C.V. 1985: Tourmaline as a petrogenetic indicator mineral: an example from the staurolite-grade metapelites from NW Maine. American Mineralogist **70**, 1–15.

Hutchinson, R.W. & Burlington, J.L. 1984: Some broad characteristics of greenstone belt gold lodes. In: Foster, R.P. (ed.): Gold, 82: the geology, geochemistry, and genesis of gold deposits, 339–371. Rotterdam: Balkema.

Kalsbeek, F. & Christiansen, F.G. 1992: Disko Bugt Project 1991, West Greenland. Rapport Grønlands Geologiske Undersøgelse **155**, 36–41.

Saager, R., Oberthür, T. & Tomschi, H.P. 1987: Geochemistry and mineralogy of banded iron-formation-hosted gold mineralization in the Gwanda greenstone belt, Zimbabwe. Economic Geology **82**, 2017–2032.

Sawkins, F.J. & Rye, D.M. 1974: Relationship of Homestake-type gold deposits to iron-rich Precambrian sedimentary rocks. Transactions of the Institute of Mining and Metallurgy **B 83**, 56–59.

Steenfelt, A. 1992: Gold, arsenic and antimony in stream sediment related to supracrustal units between Arfersiorfik and Qarajaq Isfjord (68°N to 70°30′N), West Greenland. Open File Series Grønlands Geologiske Undersøgelse **92/4**, 17 pp.

Stendal, H., Knudsen, C., Marker, M. & Thomassen, B. 1999: Gold mineralisation at Eqi, north-east Disko Bugt, West Greenland. In: Kalsbeek, F. (ed.): Precambrian geology of the Disko Bugt region, West Greenland. Geology of Greenland Survey Bulletin **181**, 129–140 (this volume).

Thomassen, B. & Tukiainen, T. 1992: Gold mineralisation in Precambrian supracrustal rocks on southern Nuussuaq, central West Greenland: 1991 results. Open File Series Grønlands Geologiske Undersøgelse **92/3**, 31 pp.

Thorpe, R.I. & Franklin, J.M. 1984: Chemical-sediment-hosted gold. In: Eckerstrand, O.R. (ed.): Canadian mineral deposit types: a geological synopsis. Geological Survey of Canada Economic Geology Report **36**, 29 only.